

## SIMULATED AND EXPERIMENTAL RESULTS FOR A HYDRAULIC ACTUATOR CONTROLLED BY TWO HIGH-SPEED ON/OFF SOLENOID VALVES

David T. Branson III<sup>1</sup>, John H. Lumkes Jr.<sup>2</sup>, Kitti Wattananithiporn<sup>3</sup> and Frank J. Fronczak<sup>3</sup>

<sup>1</sup>University of Bath, Department of Mechanical Engineering, BA1 1AL Bath, United Kingdom

<sup>2</sup>Purdue University, Agricultural and Biological Engineering, 225. South University St., West Lafayette, IN, USA

<sup>3</sup>University of Wisconsin-Madison, Mechanical Engineering, 1513 University Avenue, Madison, WI, USA  
d.branson@bath.ac.uk, lumkes@purdue.edu, fronczak@engr.wisc.edu

---

### Abstract

Research was completed to investigate the use of high-speed on/off valves in the control of a hydraulic actuator. This work was completed as part of efforts to improve the accuracy and smoothness of travel for a six-degree-of-freedom testing machine. A mathematical representation of the system was developed that correctly predicted experimental results when a single command pulse was sent to the valves. For experiments involving a series of pulses to the valves the simulated and experimental results generally agreed at lower duty cycles, however, at higher duty cycles there was some separation in the results due to assumptions made in the simulation.

**Keywords:** on/off valves, digital hydraulics, position control, simulation and modelling

---

### 1 Introduction

The use of high speed on/off valves is the topic of current research at universities around the world. Such valves, distributed throughout the hydraulic system and in place of traditional directional control valves, may reduce metering losses, improve controller bandwidth, and in some cases redirect energy that normally would be dissipated over a control valve (Andruch and Lumkes, 2008). In a more restricted application (i.e. single actuator with a decoupled metering valve) the possible energy savings are already well documented and demonstrated (Shenouda, 2006; Song and Yao, 2002; Elfving and Palmberg, 1997; Hu et al., 2001; Jansson and Palmberg, 1990). Similar to this approach is the use of multiple on/off valves in a parallel configuration to provide discrete binary flow changes and minimal metering losses (Laamanen et al., 2004).

Another method of reducing metering losses and achieving smooth control is through the use of displacement control, differing from this research in that no metering valves are used and the power supplied to the system is controlled at the source (Rahmfeld and Ivantysynova, 2001).

A particular challenge of using high speed on/off valves is achieving smooth control in an inherently high gain (pressure to force gain) system. One of the pri-

mary advantages of hydraulic cylinders, very large forces in a small package, also presents the largest challenge in using high speed on/off valves as the primary method of cylinder position control. Whereas it is straightforward to use pulse-width-modulation (PWM) meter-less control in electrical systems where the current to force (or torque) gain is much lower and the inertial to compliance (inductance to capacitance) ratio is very high, the opposite is true in hydraulic systems. The larger equivalent compliance of hydraulic systems leads to additional losses not found in electrical analogies (Scheidl et al., 2005).

In an electrical system, a switch controls the voltage (i.e. pressure) which then "accelerates" the charge, resulting in charge flow (electrical current), and finally force (or torque) at the actuator. The force (effort) depends on the current (flow), while in hydraulics the force (effort) depends directly on the pressure (also an effort). Hydraulic switching control methods are typically controlling a flow source into relatively stiff systems with rapid pressure rise rates, leading to rapid force changes and noise. The options are to make the system more compliant (add an accumulator), add inertia (again increasing the time constant), or use faster switching hydraulic valves. Actively controlling flow in and out of an accumulator using high speed valves is one method attempting to balance these design tradeoffs (Juhala et al., 2007).

To better optimize the behavior of systems using

---

This manuscript was received on 30 April 2008 and was accepted after revision for publication on 4 July 2008

high speed on/off valves it is important to understand the underlying physics and generate system level models able to be used as a design tool. The fundamental goal of this research is to develop a mathematical model to represent a hydraulic actuator controlled by two on/off valves. This paper first describes the simulation model and assumptions made in its formulation. It then considers the experimental system used to test the modeled system. Finally the simulation is validated by comparison to experimental results. In the future the validated model can be used to evaluate advanced control methods and changes in the parameters of the physical system. Similar work has examined the effect of using a parallel configuration of on/off valves on pressure peaks during cylinder control (Laamanen et al., 2007), and using a multifunctional integrated valve to control asymmetrical cylinders (Yao et al., 2005).

## 2 The Physical System

The physical system is based on one of six hydraulic cylinders used in a six-degree-of-freedom testing machine (Hage, 1997). Along with the hydraulic power supply components the system also includes two high-speed on/off solenoid valves, two variable orifices, and the necessary transport hoses and fittings (Fig. 1). An additional accumulator was added on the supply side of valve 1 to help maintain constant fluid pressure and flow.

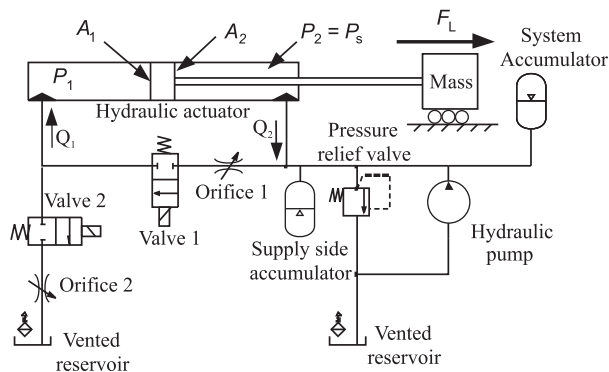


Fig. 1: Hydraulic system schematic

### 2.1 Hydraulic Power Supply and Transport Hoses

The hydraulic power supply consists of a hydraulic pump, pressure relief valve, and accumulator. The pump is driven at 1200 rpm and has a fixed displacement of 58 cc/rev. The fluid from the supply is transported to the valves and actuator through 6.35 mm diameter rubber hoses capable of operating up to 345 bar.

### 2.2 Actuator

The hydraulic actuator is a double-acting single ended actuator with an integral potentiometer position sensor for feedback control. The cylinder has a 0.15 m stroke, 12.6 mm piston radius and 2:1 area ratio.

### 2.3 High-Speed On/Off Valves

Flow control is accomplished using normally closed electro-hydraulic on/off solenoid control valves (Apitech VE5001 series) and manually adjustable orifices as shown in Fig. 1. The orifices are used to reduce the flow through the valves and adjust the actuator movement resolution. The orifices also act as a means to equalize flow in both directions due to differences in the valve manifolds, lengths of transport hoses, and fittings on each side of the actuator.

### 2.4 System Operation

To control the direction of actuator travel the solenoid valves are actuated as shown in Table 1. When valve 1 opens and valve 2 is closed, pressure in the piston side,  $P_1$ , will initially increase causing the actuator to extend.  $P_1$  will then decrease until the piston reaches constant speed and the inertia forces due to acceleration become zero. When valve 2 opens and valve 1 is closed, pressure in the annulus side,  $P_2$ , assumed equal to the supply pressure,  $P_s$ , will initially drop and fluid flows to the reservoir causing the actuator to retract. In this case  $P_1$  will then increase until the piston moves at a constant velocity. In the case that both valves are opened, all hydraulic fluid from the pump will pass directly to the reservoir allowing the piston to float freely.

Table 1: Valve operation truth table

Valve 1	Valve 2	Operation
On	Off	Extension (Right)
Off	On	Retraction (Left)
On	On	Float
Off	Off	Hold Position

## 3 Simulation

### 3.1 Assumptions

To simplify the system several assumptions were made. First, the supply pressure,  $P_s$ , was assumed to be constant and leakage flow in the actuator neglected. Also, through experimentation the effective bulk modulus,  $\beta_e$ , was estimated to be  $6.9 \times 10^8$  Pa due to the effect of entrained air in the system.

Furthermore, the relationships between flow and pressure drop across the orifices, manifolds, and valves are not modeled independently. Through experimentation the overall flow response versus pressure drop and number of orifice turns during extension of the actuator with the valves fully open was found to be

$$Q_s + Q_2 = (0.43N_1 - 0.026)\Delta P^{(0.77-0.29N_2)} \quad (1)$$

and during retraction

$$Q_R = (0.42N_2 - 0.024)\Delta P^{(0.76-0.27N_1)} \quad (2)$$

where  $Q_s$  is the supply flow,  $Q_2$  is the flow leaving the rod side of the cylinder, and  $Q_R$  is the flow to the reservoir through valve 2 as shown in Fig. 2. Also,  $N_1$  is the

number of turns for orifice 1,  $N_2$  the number of turns for orifice 2, and  $\Delta P$  the pressure drop across the flow path where  $\Delta P = P_1 - P_s$ .

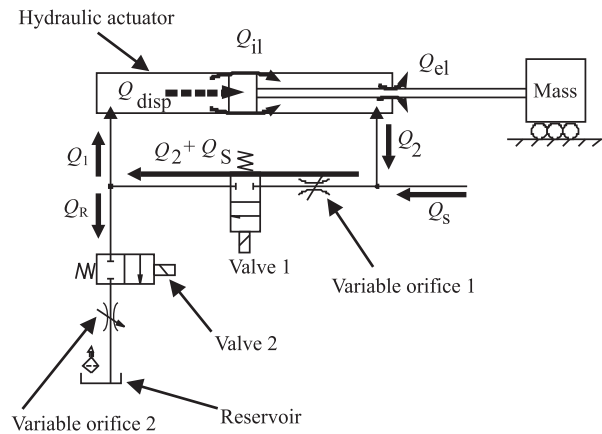


Fig. 2: Circuit flow definitions

The actuator damping coefficient,  $C_a$ , was determined experimentally from pressure data and the force relationships in the actuator when moving at constant velocity as

$$C_a = \frac{P_1 A_1 - P_s A_2 - f}{\dot{x}_a} \quad (3)$$

where  $A_1$  is the area of the piston side,  $A_2$  is the area of rod side,  $\dot{x}_a$  is the velocity of the piston, and  $f$  is the friction force represented by

$$f = \begin{cases} f_d \text{sign}(\dot{x}_a) & ; \dot{x}_a \neq 0 \\ f_d \text{sign}(f_a) & ; \dot{x}_a = 0 \text{ and } |f_a| > f_d \\ f_a & ; \dot{x}_a = 0 \text{ and } |f_a| \leq f_d \end{cases} \quad (4)$$

where  $f_d$  is the experimentally determined friction force (Magnus, 1999), and  $f_a$  is the static friction force defined by

$$f_a = P_1 A_1 - P_s A_2 - F_L \quad (5)$$

While both static and viscous friction terms are included in the model, most work with hydraulic actuators has found actuator friction to be nonlinear pressure and velocity dependant in nature (Karnopp, 1985; Tomlinson et al., 2003; Zyada and Fukada, 2001; Bonchis et al., 1999). Because the actuator is repeatedly starting and stopping the effects of friction may be higher than originally suspected due to changes in the system pressure and velocity. Further experimental testing would be needed to clarify these effects on the system and include them in future system models.

It was also necessary to determine a relationship for the valve's poppet position versus time,  $t$ . First the time lag at which the valve would begin to open or close was determined experimentally by looking at the changes in system pressure after sending a command signal to the valves (Fig. 3). Pressure was used to determine the valve delay times because due to inertia effects, changes in pressure occur at faster speeds than changes in actuator position. It was found that the valve had an opening delay time,  $T_{od}$ , of 4 ms, and a closing delay time,  $T_{cd}$ , of 2 ms.

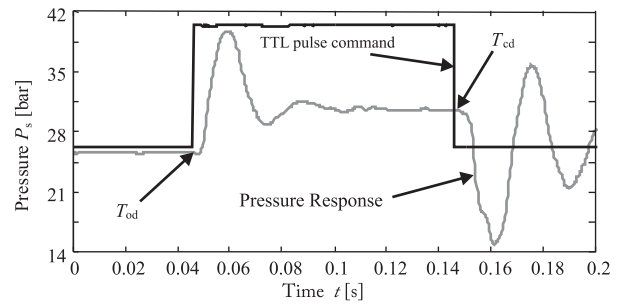


Fig. 3: Pressure response of the Apitech valve to TTL command pulse

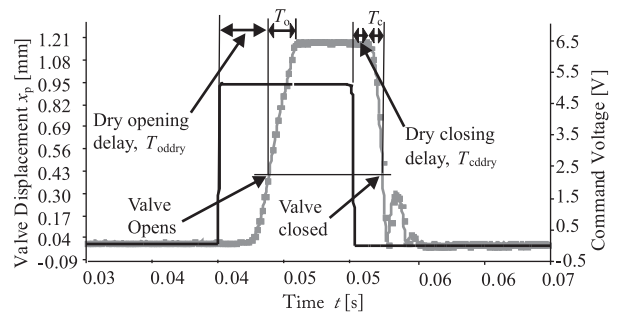


Fig. 4: Transient response of the on/off valve poppet (no hydraulic fluid in valve; 10 ms command pulse)

Next, an investigation into the transient response of the valve's poppet position was accomplished by attaching a proximity sensor to the bottom of the valve. However, because the seat of the valve needed to be taken off to allow access for the sensor this investigation was limited in that no hydraulic fluid was in the valve. Figure 4 shows the transient response of the valve when measured without hydraulic fluid. Flow will move through the valve when the poppet displacement,  $x_p$ , has surpassed  $x_{p\text{flow}} = 0.4$  mm. After which the poppet will continue to move until it reaches a maximum travel,  $x_{p\text{max}}$ , of 1.15 mm. It was found from these experiments that a linear model would accurately represent the dynamic poppet response where  $T_o$  and  $T_c$  represent the additional time that the poppet takes to completely open or close respectively once the poppet has displaced enough to allow flow.

Figure 5 shows the 1st order model of the valve used in the simulation. Experimental results showed a total opening time,  $T_o + T_{od}$ , of 6 ms, and closing time,  $T_c + T_{cd}$ , of 4 ms. The valve displacement is then converted into a coefficient,  $K_{\text{vout}}$ , from 0 to 1 based on the transient response from Fig. 4.

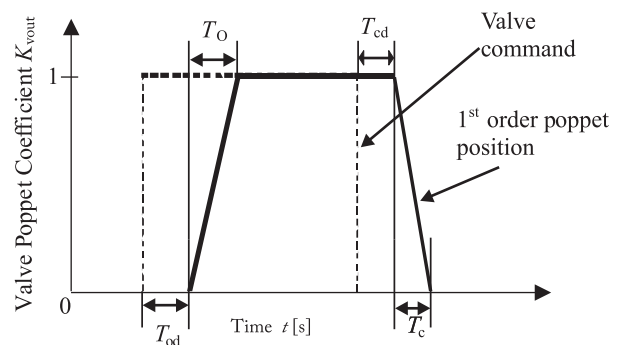


Fig. 5: Linear order model of poppet valve position

$$K_{\text{vout1}}(t) = \frac{x_{\text{p1}}(t) - x_{\text{pflow}}}{x_{\text{pmax}} - x_{\text{pflow}}} \quad (6)$$

and  $K_{\text{vout2}}(t) = \frac{x_{\text{p2}}(t) - x_{\text{pflow}}}{x_{\text{pmax}} - x_{\text{pflow}}}$

where  $K_{\text{vout}}$  is equal to 0 when  $x_{\text{p}}$  is less than or equal to  $x_{\text{pflow}}$ , and combining the effects of  $T_o$ ,  $T_{od}$ ,  $T_c$ , and  $T_{cd}$ .

### 3.2 Simulation Model

The system model was divided into three subsystems (controller, valve driver, and hydraulic components) and modeled using Matlab Simulink as shown in Fig. 6. The model parameters listed in Table 2 were then used in the simulations.

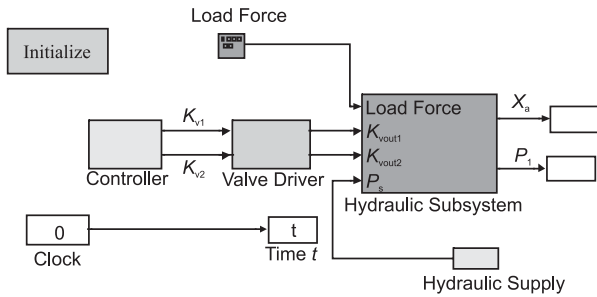


Fig. 6: Main user interface for Simulink model

Table 2: System parameter values

Description	Symbol	Value	Units
Supply pressure	$P_s$	52	bar
Effective bulk modulus	$\beta_e$	$6.9 \times 10^8$	Pa
Actuator damping coefficient	$C_a$	1400	Ns/m
Actuator mass	$M_t$	1.9	kg
Piston side area	$A_1$	500	mm <sup>2</sup>
Rod side area	$A_2$	250	mm <sup>2</sup>
Load force on the actuator	$F_L$	0	N
Volume of fluid on the piston side	$V_0$	0.1	L
Experimental friction force	$f_d$	36	N

#### 3.2.1 Valve Driver Subsystem

Figure 7 shows the Simulink models used in the valve driver subsystem.  $K_{v1}$  and  $K_{v2}$  represent the on/off command from the controller that needs to be converted to poppet position coefficients  $K_{\text{vout1}}$  and  $K_{\text{vout2}}$ . This conversion method is based on the simplified transient model for the opening and closing characteristics of the poppet valve discussed in Section 3.1.

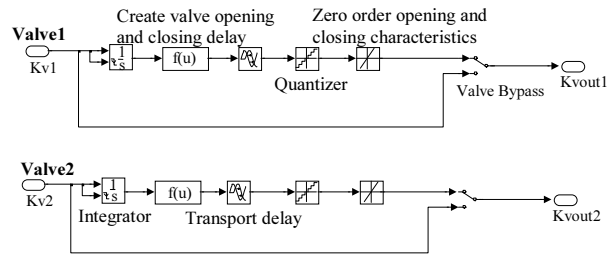


Fig. 7: Valve characteristics subsystem

#### 3.2.2 The Hydraulic Subsystem

The hydraulic subsystem includes models for the actuator and flow calculations as shown in Fig. 8.

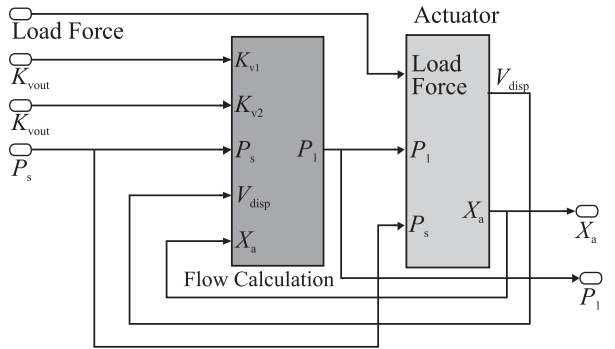


Fig. 8: Hydraulic subsystem

##### 3.2.2.1 Flow calculation subsystem

The flow subsystem outputs the value for  $P_1$  based on inputs for supply pressure,  $P_s$ , position of the actuator relative to the centre,  $x_a$ , volume of fluid displaced in the piston side due to actuator movement,  $V_{\text{disp}}$ , and valve poppet position coefficients,  $K_{\text{vout1}}$  and  $K_{\text{vout2}}$  for valves 1 and 2 respectively.  $P_1$  is determined using the effective bulk modulus,  $\beta_e$ , compressibility flow,  $Q_{\text{comp}}$ , and effective volume as

$$P_1 = \int \left( \frac{\beta_e Q_{\text{comp}}}{V_0 + V_{\text{disp}}} \right) dt \quad (7)$$

where  $V_0$  is the volume of fluid on the piston side containing the hydraulic fluid in the hoses and piston side of the actuator when the actuator is in the middle position and valves closed.  $V_{\text{disp}}$  is equal to  $A_1 x_a$ , and  $P_1$  is limited to ensure that the pressure does not go below 0 bar.

Because hydraulic fluid is not infinitely stiff in nature and will compress under pressure, this effect must be accounted for in the flow calculations.  $Q_{\text{comp}}$  can be found by assuming flow continuity and conservation of mass where

$$Q_{\text{comp}} = Q_1 - Q_{\text{disp}} - Q_{\text{il}} - Q_{\text{el}} \quad (8)$$

and  $Q_1$  is the flow rate into the piston side of the cylinder,  $Q_{\text{disp}}$  is the flow rate due to the displacement of the piston ( $Q_{\text{disp}} = A_1 \dot{x}_a$ ), and  $Q_{\text{il}}$  and  $Q_{\text{el}}$  are the flows due to internal and external leakage respectively (Fig. 2). The simulation assumes that the internal and external

leakages are small and these terms may be ignored. Equation 6 may be applied regardless of direction of travel in the actuator, however, care must be taken to account for any sign changes.

To find  $Q_1$  consider the flow across the valves during retraction and extension of the actuator (Eq. 1 and 2), and the linearized poppet opening profile approximations for the valve from Section 3.1. The magnitude of flow across the valves is assumed to be proportional to  $K_{vout1}$  and  $K_{vout2}$ . Modifying Eq. 1 and 2 to include  $K_{vout1}$  and  $K_{vout2}$  results in the following relationships for flow in extension

$$Q_s + Q_2 = K_{vout1} (0.43N_1 - 0.026) \Delta P^{(0.77-0.29N_2)} \quad (9)$$

and retraction

$$Q_R = K_{vout2} (0.42N_2 - 0.024) \Delta P^{(0.76-0.27N_1)} \quad (10)$$

$Q_1$  can then be determined using continuity and mass conservation principles as applied to the manifold and neglecting leakage.

$$Q_1 = (Q_s + Q_2) - Q_R \quad (11)$$

### 3.2.2.2 Actuator subsystem

The equation of motion for the actuator is obtained using Newton's second law, where the forces acting on the piston are due to pressures  $P_1$  and  $P_s$ ,  $C_a$ ,  $F_L$ , and any forces due to friction,  $f$ .

$$M_t \ddot{x}_a = P_1 A_1 - P_s A_2 - C_a \dot{x}_a - f - F_L \quad (12)$$

where  $\ddot{x}_a$  is the actuator acceleration and  $\dot{x}_a$  is the actuator velocity.

To find  $\dot{x}_a$  and  $x_a$  first solve Eq. 10 to find  $\ddot{x}_a$ , and then integrate the result as a function of time. In the simulation the velocity integrator is limited to ensure that  $x_a$  does not exceed the displacement range of the experimental cylinder. If the calculated actuator position exceeds the limits then switch functions will set  $\dot{x}_a$  and  $\ddot{x}_a$  to zero stopping the piston without any dynamic reaction.

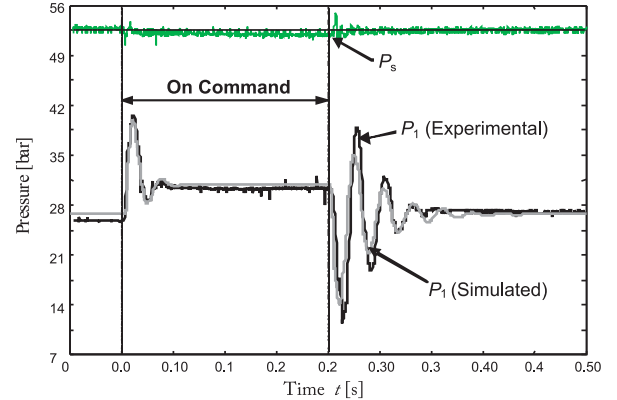
## 4 Results

The characteristics of the hydraulic system were investigated experimentally and theoretically for single and multiple on/off pulse commands to the valves using a supply pressure of 52 bar. The results of the tests were then compared to validate the simulation model.

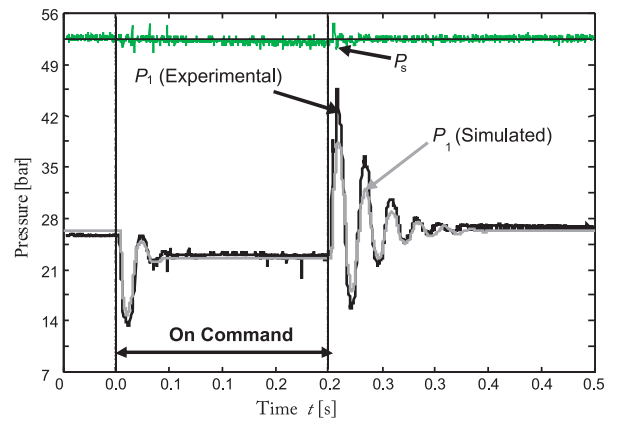
### 4.1 Single Pulse Tests

A comparison between the simulated and experimental pressure results for a single pulse to the valves are shown in Fig. 9a and 9b. There is strong agreement between the simulated and measured responses. There are only minor differences in the damping rate between the simulation and experimental data. Other differences between the simulated and experimental results are due to fluctuations in  $P_s$  not modeled in the simulation.

Although the accumulator in the system should have helped to maintain constant pressure over the short duration of each test, once the valves opened the supply pressure still decreased due to flow restrictions in the transport hoses and fittings. However, the resulting simulated versus experimental results were felt to be sufficient at this time for controller development and no further work was completed



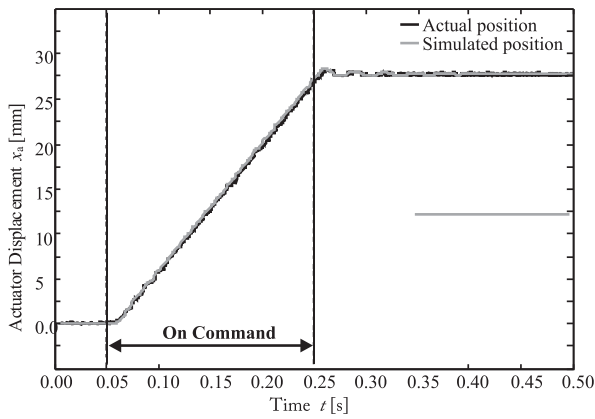
a) Extension



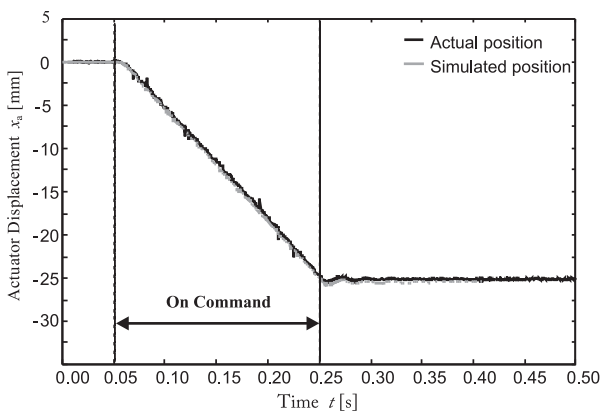
b) Retraction

**Fig. 9:** Simulated and experimental comparison of pressure on the piston side (52 bar supply pressure,  $1/4$  turn orifice opening, 22.7 kg mass, and cylinder in middle)

A comparison of the piston displacements show that they are in agreement (Fig. 10a and 10b), where minor velocity differences are due to the drop in  $P_s$ . Additionally, the displacement of the poppet is dependant upon the current output of the valve driver. This was controlled by programmed voltages, which could not always be held constant due to limitations in the experimental valve driver. It was found that any small fluctuation of the voltage, of even a few mV, greatly affected the valve poppet position.



a) Extension



b) Retraction

**Fig. 10:** Simulated and experimental comparison of actuator displacement (52 bar supply pressure, 1/4 turn orifice opening, 22.7 kg mass, and cylinder starting in middle)

#### 4.1.1 Sensitivity Analysis

The effects of changing system parameters for single pulse tests were also considered. These included varying the initial position of the cylinder, pulse length, supply pressure, and orifice opening.

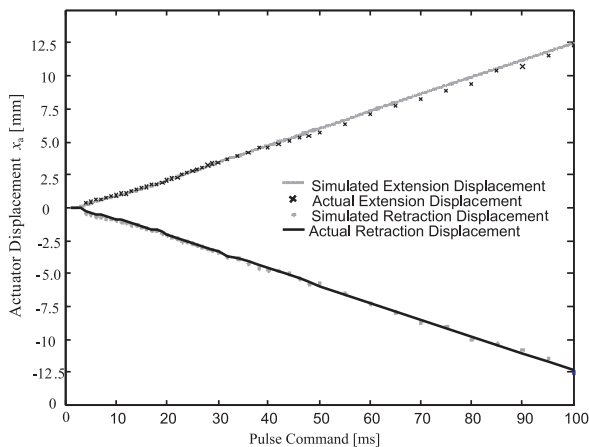


**Fig. 11:** Relationship between actuator displacement and length of pulse command (52 bar supply pressure, 1/4 turn orifice opening, 22.7 kg mass, and cylinder starting in middle position)

The compressible volume, and therefore the effective spring rate, varies with actuator position. As ex-

pected, it was found that decreasing the extension length of the actuator would slightly increase the overshoot amplitude for the position and pressure results. Also, the system natural frequency was higher when the piston was fully retracted. However, the overall effect of changing actuator position was negligible for both simulated and experimental results.

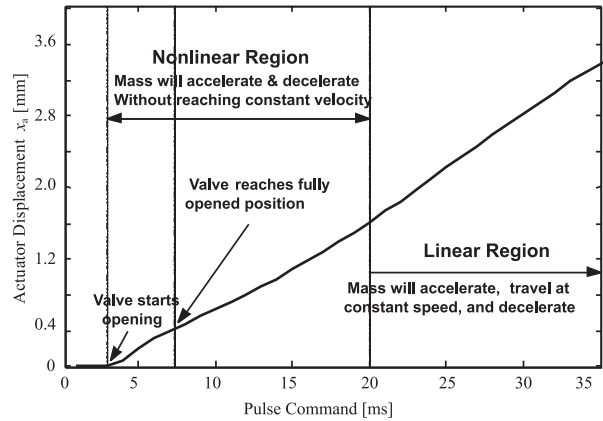


**Fig. 12:** Linear and nonlinear regions for the relationship between actuator displacement and pulse command length (52 bar supply pressure, 1/4 turn orifice opening, 22.7 kg mass, and cylinder extending from middle)

Increasing the pulse command length to the valve resulted in a linear increase in final position as shown in Fig. 11. However, for shorter pulse lengths the response of the actuator position was nonlinear as shown in Fig. 12. This is because it will take some time to fully accelerate the mass to constant velocity. If the valve does not stay open long enough to achieve constant actuator velocity then its final displacement is nonlinear in nature.

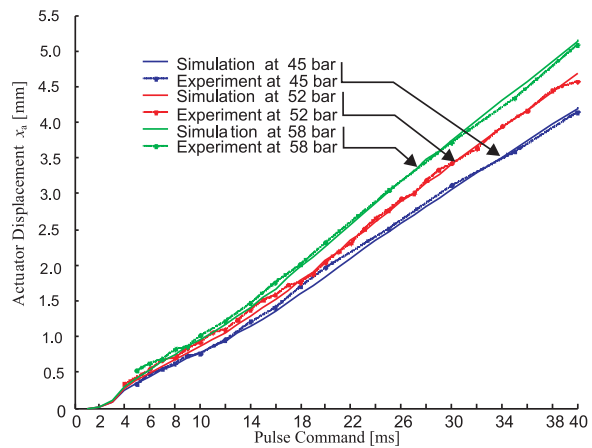


**Fig. 13:** Effect of changing supply pressure on actuator displacement (1/4 turn orifice opening, 22.7 kg mass, and cylinder extending from middle)

Figure 13 shows the effects of varying supply pressure. It can be seen that increasing the supply pressure increases the maximum flow rate across the valves causing the piston to travel farther for a given pulse length. Changing the orifice opening can also have a significant effect on the final actuator displacement. Figure 14 shows that by increasing the number of turns,

and therefore the size of the orifice opening, there is a corresponding increase in the flow rate and actuator displacement.

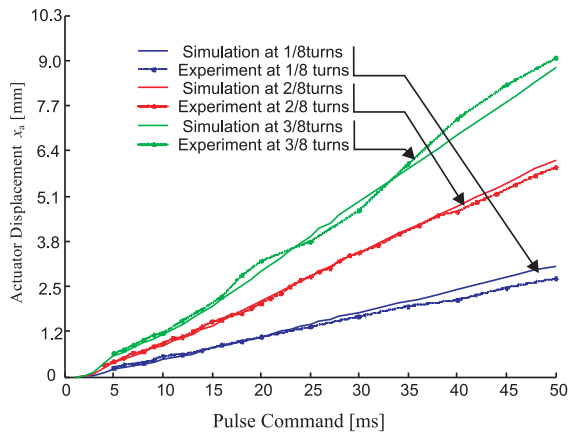


**Fig. 14:** Effect of changing orifice opening on piston displacement (52 bar supply pressure, 22.7 kg mass, and cylinder extending from middle)

#### 4.2 Multiple Pulse Experiments

A series of PWM commands were sent to the valves and the results evaluated. As expected, it was found that by varying the signal duty cycle (the ratio in percentage between the length of signal “on” versus “off” for a given pulse train frequency), the average velocity associated with the actuator will vary. The PWM frequency is a function of valve switching speeds and a tradeoff between ripple and efficiency. Increasing the frequency will reduce efficiency since the valve transition time becomes a larger percentage of the total cycle time, leading to more metering losses, and compressibility losses increase (Batdorff and Lumkes, 2006).

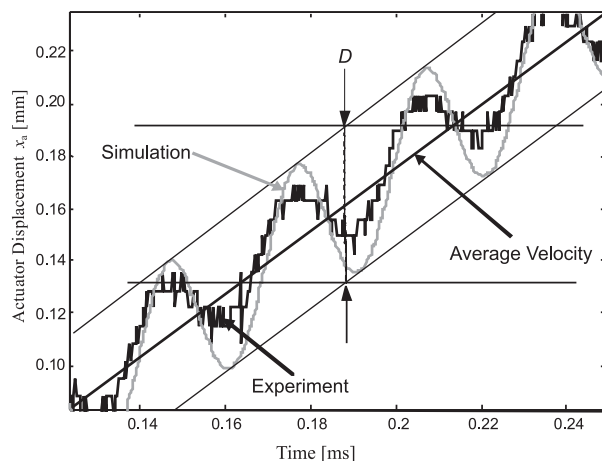


**Fig. 15:** Displacement, smoothness and average actuator position due to 33 Hz pulse train at 40 % duty cycle (52 bar supply pressure, 1/4 turn orifice opening, 22.7 kg mass, and cylinder extending from middle)

Average actuator velocity is found by measuring the mean slope of actuator displacement versus time over a series of command pulses as shown in Fig. 15.

A plot of the response for average piston velocity versus percent duty cycle is shown in Fig. 16. It can be seen that there is a good correlation between the simu-

lated and experimental results up to a duty cycle of around 40 %, after which some separation will occur between the two. Above 80 % duty cycle the pulse train command results in the maximum achievable actuator velocity.

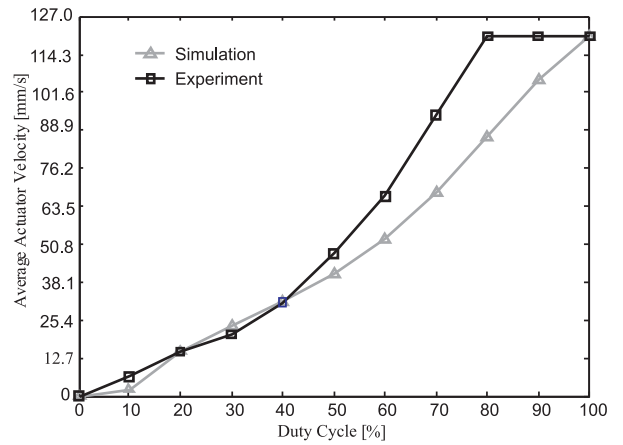


**Fig. 16:** Pulse command duty cycle versus average actuator velocity (52 bar supply pressure, 1/4 turn orifice opening, 22.7 kg mass, and 33 Hz pulse train)

Smoothness is a key function used to determine the accuracy and stability of a system response and is defined by the factor  $1/D$ , where  $D$  is the actuator fluctuation from Fig. 15. It can be seen in Fig. 17 that the system has greater fluctuations over the middle range duty cycles, while there is very little fluctuation in the experimental data above approximately 80 %. This seems to indicate that the valve may not be completely opening at the smaller duty cycles, and is not completely closing at higher duty cycles. At the low and high duty cycle endpoints the flow is thus not interrupted by the opening and closing of the valves and the actuator travel is smoother.

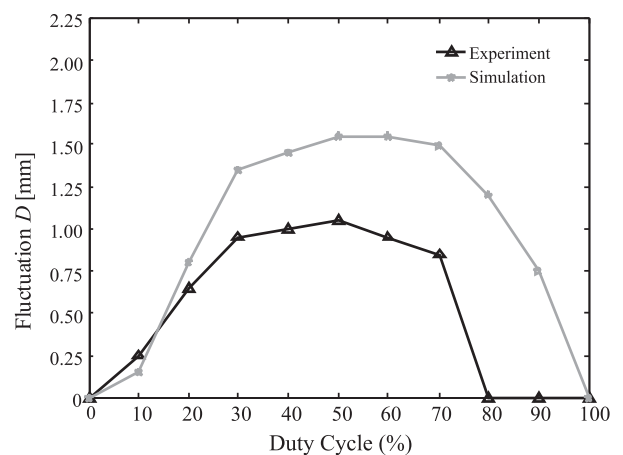


**Fig. 17:** Plot of the fluctuation response at varying duty cycles (52 bar supply pressure, 1/4 turn orifice opening, 22.7 kg mass, and 33 Hz pulse train)

## 5 Conclusions

This paper shows the development of a simulation model for a hydraulic actuator controlled by two high-speed on/off valves. The model is then verified against experimental results using single and multiple command pulses to the control valves. Good agreements between the experimental and simulated results were found for single pulse commands to the valves. This included when adjustments were made to system parameters for starting actuator position, system pressure, and orifice opening.

For experiments involving PWM commands to the valves the simulated and experimental results agreed at lower duty cycles, but did not have very good agreement at higher duty cycles. This is due to the fact that several assumptions were made to simplify the model that limited its performance.

This simulation can be used to predict the response of similar hydraulic systems, and early results show that faster acting valves result in smoother and more accurate movements of the piston. Further work has also been completed into the development of feedback control methods for such a system using Bang-Bang, Pulse Duration Modulation (PDM), and floating strategy with PID control to improve actuator travel smoothness and accuracy (Wattananithiporn, 2002). Additional work developing improved control methods in digital hydraulic systems is still needed.

## Nomenclature

$A_1$	Piston side area of piston	[m <sup>2</sup> ]
$A_2$	Rod side area of piston	[m <sup>2</sup> ]
$\beta_e$	Effective bulk modulus	[Pa]
$C_a$	Actuator damping coefficient	[Ns/m]
$D$	Actuator fluctuation	[m]
$f$	Friction force	[N]
$f_a$	Static friction force	[N]
$f_d$	Experimental friction force	[N]
$F_L$	Load force on the actuator	[N]
$K_v$	On/Off command to valve	
$K_{v1}$	On/Off command to valve 1	
$K_{v2}$	On/Off command to valve 2	
$K_{vout}$	Valve displacement coefficient	
$K_{vout1}$	Valve 1 poppet displacement coefficient	
$K_{vout2}$	Valve 2 poppet displacement coefficient	
$M_t$	Actuator mass	[kg]
$N_1$	Number of orifice turns on orifice 1	
$N_2$	Number of orifice turns on orifice 2	
$P_1$	Piston side pressure	[bar]
$P_2$	Annulus side pressure	[bar]
$P_s$	Supply pressure	[bar]
$\Delta P$	Pressure drop across the flow path	[bar]
$Q_1$	Flow into piston side	[L/min]
$Q_2$	Flow out of rod side	[L/min]
$Q_{comp}$	Flow due to compression of fluid	[L/min]
$Q_{disp}$	Flow due to displacement of piston	[L/min]
$Q_{el}$	Flow due to external leakage	[L/min]

$Q_{il}$	Flow due to internal leakage	[L/min]
$Q_R$	Flow to the reservoir through valve 2	[L/min]
$Q_s$	Supply Flow	[L/min]
$t$	Time	[s]
$T_c$	Closing time of valve	[s]
$T_{cd}$	Closing delay time of valve	[s]
$T_{cddry}$	Closing delay time of valve without hydraulic fluid present	[s]
$T_o$	Opening time of valve	[s]
$T_{od}$	Opening delay time of valve	[s]
$T_{oddry}$	Opening delay time of valve without hydraulic fluid present	[s]
$V_{disp}$	Volume of fluid on the piston side displaced by actuator movement	[L]
$V_0$	Volume of fluid on the piston side when the actuator is in the middle position	[L]
$x_a$	Actuator position (0 in middle position)	[m]
$\dot{x}_a$	Actuator velocity	[m/s]
$\ddot{x}_a$	Actuator acceleration	[m/s <sup>2</sup> ]
$x_p$	Valve poppet position	[m]
$\dot{x}_p$	Valve poppet velocity	[m/s]
$\ddot{x}_p$	Valve poppet acceleration	[m/s <sup>2</sup> ]
$x_{pflow}$	Poppet displacement at which flow begins	[m]
$x_{pmax}$	Max poppet displacement	[m]

## References

- Andruch, J. and Lumkes, J.** 2008. A Hydraulic System Topography with Integrated Energy Recovery and Reconfigurable Flow Paths Using High Speed Valves. *Proceedings of the 51st National Conference on Fluid Power (NCFP)*, March, NCFP I08-24.1, pp. 649-657.
- Batdorff, M. and Lumkes, J.** 2006. Virtually Variable Displacement Hydraulic Pump Including Compressibility And Switching Losses. *Proceedings of the 2006 ASME-IMECE*, Paper No. IMECE2006-14838.
- Bonchis, A., Corke, P. I. and Rye, D. C.** 1999. A Pressure-based, Velocity Independent, Friction Model for Asymmetric Hydraulic Cylinders. *IEEE International Conference on Robotics and Automation*. Detroit, MI.
- Elfving, M. and Palmberg, J. O.** 1997. Distributed Control of Fluid Power Actuators - Experimental Verification of a Decoupled Chamber Pressure Controlled Cylinder. *4th International Conference on Fluid Power*.
- Hage, R.** 1997. *Development of a Parallel Mechanism Test Machine with Six-Degree-of-Freedom Position and Force Control*. Ph.D. Thesis. University of Wisconsin-Madison.



- Hu, H., Zhang, Q. and Alleyne, A.** 2001. Multi-function Realization of a Generic Programmable E/H Valve using Flexible Control Logic. *Proceedings of the Fifth International Conference on Fluid Power Transmission and Control*. International Academic Publishers, Beijing, China, pp. 107-110.
- Jansson, A. and Palmberg, J.-O.** 1990. Separate Control of Meter-in and Meter-out Orifices in Mobile Hydraulic Systems. *SAE technical Paper Series*, no. 901583.
- Juhala, J., Kajaste, J. and Pietola, M.** 2007. Transient Pressure Control in Digital Hydraulic Systems. *Tenth Scandinavian Conference on Fluid Power, SICFP'07*.
- Karnopp, D.** 1985. Computer Simulation of Stick-Slip Friction in Mechanical Dynamic Systems. *Transactions of the ASME Journal of Dynamic Systems, Measurement, and Control*, 107(1), pp. 100-103.
- Laamanen, A., Siivonen, L., Linjama, M. and Vilenius, M.** 2004. Digital Flow Control Unit-an Alternative for a Proportional Valve? *Power Transmission and Control*, PTMC2004, pp. 297-308.
- Laamanen, A., Linjama, M. and Vilenius, M.** 2007. On the Pressure Peak Minimization in Digital Hydraulics. *Tenth Scandinavian Conference on Fluid Power, SICFP'07*.
- Magnus, B.** 1999. *Simulation Model for a Hydraulic Actuator Controlled by Two High-Speed On/Off Solenoid Valves*. Independent Study Report, University of Wisconsin-Madison.
- Rahmfeld, R. and Ivantysynova, M.** 2001. Displacement Controlled Linear Actuator with Differential Cylinder- a way to save Primary Energy in Mobile Machines. *Fifth International Conference on Fluid Power Transmission and Control (ICFP)*. Hangzhou, China.
- Scheidl, R., Manhartsgruber, B., Mikota, G. and Winkler, B.** 2005. State of the Art in Hydraulic Switching Control-Components, Systems, Applications. *Proceedings of the Ninth Scandinavian International Conference on Fluid Power, SICFP'05*.
- Shenouda, A.** 2006. *Quasi-Static Hydraulic Control Systems and Energy Saving Potential Using Independent Metering Four-Valve Assembly Configuration*. PhD Thesis. Georgia Institute of Technology.
- Song, L. and Yao, B.** 2002. Energy-Saving Control of Single-Rod Hydraulic Cylinders with Programmable Valves and Improved Working Mode Selection. National Fluid Power Association and Society of Automotive Engineers. *Proceedings of the 49th National Conference on Fluid Power (NCFP)*, March, NCFP 102-2.4/SAE OH 202-01-1343, pp. 81-90.
- Tomlinson, S. P., Cooke, R. W. and Cosserat, D. C.** 2003. A computationally efficient technique for modelling velocity-dependent sliding friction. *Proc. Instn Mechanical Engineers Part I: Journal of Systems and Control Engineering*, 217(I), pp. 139-146.
- Wattananithiporn, K.** 2002. *Control of a Hydraulic Actuator Using High-Speed On/Off Valves*. Masters Thesis. University of Wisconsin-Madison.
- Yao, J., Kong, X., Shan, D., Gao, Y., Han, D. and Zhang, Q.** 2005. Study on using a Multifunctional Integrated Valve in Controlling an Asymmetric Hydraulic System. *Proceedings of the 50th National Conference on Fluid Power (NCFP)*, March, NCFP 105-15.1, pp. 585-593.
- Zyada, Z. and Fukuda, T.** 2001. Identification and Modeling of Friction Forces at a Hydraulic Parallel Link Manipulator Joints. *40th Annual Conference of the Society-of-Instrument-and-Control-Engineers (SICE)*. Nagoya, Japan.



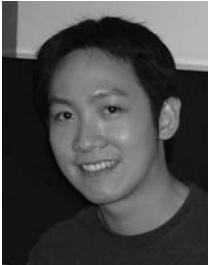
**David T. Branson III**

David received his undergraduate and Masters degrees in Mechanical Engineering from the University of Wisconsin-Madison, USA, and Ph.D. from the University of Bath, UK. Since 2006 he has been employed by the University of Bath as a Research Officer in the centre for Power Transmission and Motion Control. His research interests include dynamic systems analysis, controls, and fluid power systems and component design.



**John H. Lumkes Jr.**

John H Lumkes Jr. received the B.S.E. degree from Calvin College in 1990, the M.S.E. from the University of Michigan-Ann Arbor in 1992, and the Ph.D. from the University of Wisconsin-Madison in 1997. From 1997-2004 he was an Assistant and Associate Professor at Milwaukee School of Engineering. In 2004 he joined Purdue University as an Assistant Professor and is active in digital hydraulics, modeling and controls, mechatronics, and advising senior design projects.



**Kitti Wattananithiporn**

Kitti completed his master's degree at the University of Wisconsin-Madison in 2002 looking at the control of hydraulic actuators using high-speed on/off valves.



**Frank J. Fronczak**

Frank Fronczak received his BS and MS from the University of Illinois and his Dr. Eng. Degree from the University of Kansas in 1977. He is a Professor of Mechanical and Biomedical Engineering at the University of Wisconsin-Madison, where he has been a member of the faculty since 1982. He is the director of the UW Fluid Power Research Laboratory and the Mechanical Systems Design Laboratory.